Synthesis and characterization of the starch/silicone composite and elaboration of its films

Coyolicaltzin Peralta-González
Universidad del Papaloapan - Campus Tuxtepec
Aurelio Ramirez-Hernandez (chino_raha@hotmail.com)
Universidad del Papaloapan - Campus Tuxtepec https://orcid.org/0000-0002-7606-3871
Gustavo Rangel-Porras
Universidad de Guanajuato Division de Ciencias Naturales y Exactas
Alejandro Aparicio-Saguilán
Universidad del Papaloapan - Campus Tuxtepec
Andrés Aguirre-Cruz
Universidad del Papaloapan - Campus Tuxtepec
Gerardo González-García
Universidad de Guanajuato Division de Ciencias Naturales y Exactas
José Eduardo Báez-García
Universidad de Guanajuato Division de Ciencias Naturales y Exactas
Delia Esther Páramo-Calderón
Universidad del Papaloapan - Campus Tuxtepec

Research Article

Keywords: composite, starch, silicone, electrical conductivity

Posted Date: March 18th, 2021

DOI: https://doi.org/10.21203/rs.3.rs-315478/v1

Abstract

Synthesis of the starch/silicone composite carried out and its structural characterization by FTIR, Raman and ^{29}Si NMR allowed to identify functional groups of the composite. The synthesis conditions were a starch/silicone mass ratio of 2.0 and a temperature of 150 ^{o}C to obtain a yield of 84.63 %. SEM analysis showed that the starch granules were covered by silicone, this caused a decrease in the crystallinity of starch. Composite films have higher thermal stability compared to native starch. Mechanical properties and electrical conductivity of the starch/silicone composite film increase with respect to starch-only films. While the crystallinity of both films is similar. The results obtained in this work indicate that starch/silicone composites can be an alternative to make films with a potential use for the packaging industry.

1 Introduction

In recent years, many investigations have been carried out on the chemical or physical modification of starch to generate new biodegradable materials with possible applications at the industrial level, for example, in the area of food and in the area of plastics, to name a few [1–4].

These investigations are mainly due to the search to synthesize biomaterials that can compete with conventional plastics to reduce environmental by the increased use of disposable plastics that are not biodegradable (around 700 million tonnes of plastic wastes worldwide) [5–6]. In this regard, biocomposites have emerged as emerging materials to replace synthetic materials in several important applications. Biocomposites are the system consisting of a matrix and a reinforcing agent that behave as a single material and have interesting mechanical, electrical, optical, thermal and barrier properties from an industrial point of view. Modified starch is one of these alternatives because it is known that the materials created from only pure starch present two primary disadvantages: an excessive rigidity and an affinity for water [7]. One of these researches studied has been the combination of starch with rubber and silicone to generate soft intelligent materials with high stability against sedimentation [8]. These types of materials are known as electrorheological (ER) because it undergoes reversible changes in their mechanical properties when subjected to an electric field [9–10]. ER materials have been studied in the last three decades and are used in actuators, dampers, clutches, hydraulic valves, high power vibrators, chucks, and torque transducers [11–12]. In these investigations the banana has not been used as a source of starch nor basic conditions to facilitate the electrostatic interaction between the starch and the silicone oil. On the other hand, banana starch contains a higher amylose content than potatoes (21 % vs. 34.5 %) and knows that amylose favors the chemical or physical modification of starch, as well as, the ability to form film. Also, plantains have an annual worldwide production of 117.9 million tons and these are grown and harvested in all seasons [13–14]. Objective of this work was to synthesize a banana starch composite with silicone using potassium hydroxide to generate biodegradable material that can compete with conventional plastics.

2 Experimental Methods

2.1 Materials

Ethylene carbonate (EC), deuterated chloroform ($CDCl_3$), dimethylsulfoxide-D_6 (DMSO-D_6), silicone oil and potassium hydroxide (KOH) were purchased from Aldrich Chemical Company. The unripe banana was a gift from the “Mundo Nuevo” farm located in Tuxtepec, Oaxaca, Mexico. The fruit does not meet the quality for direct commercialization. The isolation of the starch and the determination of its chemical composition were carried out according to the methodology proposed in the literature [15–17]. It was found that this fruit contains 91.59 % ± 0.67 starch, of which 38.0 % ± 0.39 is amylose.

2.2 Methods

2.2.1 Isolation of banana starch

The banana starch was isolated following the methodology of Ramírez-Hernández et al. [17]. After the banana peel was removed the fruit was ground in an industrial type blender, (Waring Laboratory, model CB 15). In order to prevent the oxidation of the fruit (3.6 kg) of peeled banana were milled with (6 L) of 0.3 % w/v citric acid solution. The resulting mixture was filtered using an electrical sieve (Retsch, model AS 200). Different mesh sizes (Lab. Test Sieve) were used: No. 40 (0.425 mm), 100 (0.15 mm), and 270 (0.053 mm). At each step of sieving, the product was washed with sufficient water until the aqueous solution showed no apparent starch residues. At the end of the sieving operation, the starch was allowed to precipitate overnight, Thereafter the supernatant was decanted and the starch was washed with distilled water, this process was repeated three times. Finally, the product was dried in a tray dryer (manufactured by SUSESA) at 40°C overnight. The powder obtained was sieved using a 100 mesh screen, weighed and stored in a container until use. It was found that this fruit contains 91.59 % ± 0.67 starch, of which 38.0 % ± 0.39 is amylose.

2.2.2 Synthesis of composite

The physical modification of the banana starch with silicone was carried out in a 10mL vial previously dried vial, banana starch (1.0 g), silicone (0.5–1.0 g) and potassium hydroxide (0.05 g) were charged and heated by constant stirring in an oil bath at 130–150°C for 24 h. The product obtained was washed with distilled water and dried in an oven at a temperature of 37 ℃ for a period of 24 h. To determine percentage yield of the composite was used Equation (Eq. 1):

$$\text{Percentage yield} = \frac{m_2}{m_1} * 100 \qquad (1)$$

where m_2 is the final mass and m_1 is the initial.

2.2.3 Composite films

The starch/silicone composite films were obtained using the casting method. This method consisted in the dispersion of the polymers in water at 85°C for 20 min followed by the evaporation of the water at a temperature and moisture controlled, Table 1 shows the formulations of the elaborated films.

Table 1
Composition of composite films.

Film	Starch (%)	Composite starch/silicone (%)
1	100	-
2	60	40
3	80	20
4	86	14
5	90	10

The films were obtained in duplicate for characterization and glycerol was used as an additive to facilitate the formation of the films.

2.3 Structural characterization

2.3.1 Fourier transform infrared spectroscopy (FTIR)

Infrared spectra were recorded at room temperature in a Perkin-Elmer Spectrum 100FT-IR (ATR) spectrometer with a resolution of 4 cm^{-1} and averaged over 16 scans in the range of 4000–650 cm^{-1}. The Raman spectra were recorded in the 200 ± 1900 cm^{-1} spectral range with an integration time of 60 s and were averaged over three scans.

2.3.2 NMR measurements

Nuclear magnetic resonance spectra (NMR) (^{29}Si) were measured on a Varian/Agilent 600 MHz NMR spectrometer with a frequency of 599.98 MHz with π/2 pulse of 8.7 μs. DMSO-D_6 was used as solvent and chemical shifts (ppm) were determined relative to internal TMS at 0.0 ppm or the residual signal of solvent at 2.50 ppm.

2.3.3 X-ray diffraction (XRD) and scanning electron micrographs (SEM)

X-ray diffraction patterns were collected in a 2θ range of 3 to 40, using a scan rate of 1 deg/min in a Bruker AXS D8 Advance diffractometer using a CuK radiation generator with a Ni filter, 30 mA and 40 kV.

The Scanning electron micrographs (SEM) were taken using a Philips environmental microscope ESEM XL30. Prior to viewing, samples were coated with Au-Pd for 60 seconds using a Quorum V1SOR ES sputter coater.

2.3.4 Thermal, mechanical, pasting and electrical conductivity

Differential scanning calorimetry (DSC) and thermogravimetric analysis (TGA) were conducted with simultaneous DSC/TGA using as SDT Q600 thermogravimetric analyzer. The curves were recorded in a temperature range of 26°C to 700°C at a heating rate of 20°C/min using nitrogen as the purging gas.

Mechanical tests included determination of the tensile strength, percent elongation at break and elastic modulus using a TAXT-Plus texture analyzer (Stable Micro Systems, Surrey, UK), equipped with the Exponent lite software (version 4.0), operated according to the standard method ASTM D 882-95a [18–19].

Pasting formation, dispersions at 5 % (w/v) of total solids in distilled water were prepared and placed in a rheometer (TA Instruments AR 1000-N, New Castle, USA), with a parallel plate system. The top plate was acrylic with fluted texture, 60mm in diameter, and the sample thickness was 1mm. The plate system was covered with mineral oil to avoid evaporation of the water during the test. The measurement was made during a heating cycle from 25°C to 90°C and an isothermal stage was performed for 10min; it was cooled to 25°C and maintained for 10min. A heating-cooling rate of 2.5°Cmin^{-1} and a shear rate of 50 s^{-1} were used. Then the equipment was programmed for two cycles: ascending and descending from 0.03 to 100 s^{-1}, and a third descending sweep from 100 to 0.03 s^{-1}. The data obtained from the third cycle was applied the equation of the power law of Ostwald-de Waele as a function of the shear stress (t), where g = f(t), to calculate the parameters of the consistency index (K, Pa.sn) and index of flow behavior, which defined the behavior of the fluid [18].

The electrical conductivity of the film was measured using a Börk digital multimeter and a 1.39 Volt battery. One end of the film was connected to the negative pole of the battery and the other end to the positive pole. The passage of the electric current was determined using Equation (Eq. 2):

$$\text{Passage of the electric current } (\%) = \frac{Vf}{Vi} X100 \qquad (2)$$

where V_f are the volts of the sample and V_i are the volts of the battery.

3 Results And Discussion

3.1 Synthesis and characterization of composite

The synthesis of the starch/silicone composite material was carried out and the appropriate temperature and mass ratio were determined. A yield of 84.63 % was obtained for a starch / silicone mass ratio of 2.0, a time of 24 hours and a temperature of 150°C while at temperatures of 130°C and 140°C using the same mass ratio and time, the yield was 73.67 %. Structural analysis of the composite was performed by infrared spectroscopy, Raman and NMR techniques. The FTIR spectra of the starch, silicone and of starch/silicone composite are presented in Fig. 1. Banana starch presents the typical starch signals, the stretching vibration of the hydroxyl groups (-OH) at 3300 cm^{-1}, the stretching vibration of the methylene groups (-CH_2-) at 2936 cm^{-1} and the vibration signal of flexion of the group -COC- at 994 cm^{-1}. The spectrum of the silicone shows the vibration signals of the methyl group (-CH_3) at 2962 cm^{-1} and 1250 cm^{-1}, which correspond to the stretching and deformation vibrations, respectively. The vibration signal of

the structure [-O-Si-$(CH_3)_2$-]$_n$ appears in 780 cm^{-1}. Also, the flexion vibration signals of the group -C-Si-O- and -Si-O- are observed at 1080 cm^{-1} and 1000 cm^{-1}, respectively.

In the spectrum of the composite it is observed that the two vibration signals of the hydroxyl group increase its intensity (3300 cm^{-1} and 1640 cm^{-1}) due to the electrostatic attraction between the hydroxyl group (-OH) of the starch with the oxygens of the silicone. In this spectrum, the vibration signals of silicone and starch are observed, which are similar to those reported in the literature by other researchers [20]. Raman spectrum of the starch/silicone composite (Fig. S1 in the Supplementary Information file) presents two vibrational modes of the group -Si-CH_3 in 2907 cm^{-1} and in 1296cm^{-1}. Wavenumber at 1594 cm^{-1} corresponds to the vibrational mode of the hydroxyl group (-OH), the vibration signal at 707 cm^{-1} corresponds to the Si-O-Si group and the signal at 487 cm^{-1} corresponds to the chemical bond C-O-C as reported in the literature [21–24]. ^{29}Si NMR spectrum of silicone and starch/silicone composite only show a single chemical shift at -20.62 ppm and − 19.77 ppm, respectively (Fig. 2).

This chemical shift corresponds to the monomeric unit of poly(dimethylsiloxane). Silicone spectrum has a difference of approximately one unit compared to the chemical displacement of the starch/silicone composite and its peak is sharper. This is due to the electrostatic interaction of starch with the Si-O group of the composite. This silicone signal is similar to that reported in the literature [41]. These results are in agreement with those observed in the FTIR spectra It can be concluded that the composite material was obtained and that there is only a physical interaction between starch and silicone. However, the electrostatic interactions between starch and silicone can make it possible to obtain new materials with different thermal, mechanical and physicochemical properties than their constituent components, potentiating their use in the packaging industry.

3.2 Morphological analysis by scanning electron microscopy

SEM micrographs of the banana starch granules before and after their physical interaction with silicone samples at different resolutions (200x, and 1.0 kx) (Fig. 3).

Figure 3a (resolution of 200x) shows the shape of the banana starch grain is typically elliptical-like with a size of 5–50 μm, these results are similar to those reported in the literature by other researchers [25–26]. Micrograph of the starch/silicone composite (Fig. 3b) a continuous phase (silicon matrix) could be observed in which the starch granules are enveloped apparently without changes in their structure. This can be confirmed in Fig. 3c where the micrographs show no damage to the morphology of the starch granules in the composite. The silicone covers the surface of the starch granules and forms stackings of these (Fig. 3d) which would favor their protection against possible changes in temperature and chemical substances. This coating further facilitates electrostatic interaction between the OH groups of the starch with the Si-O group of the silicone. There are several works of formulations in where starch combine with silicones for the purpose of explicitly seeking hydrophobicity. The reaction of silicones with starch under basic conditions, leads to starch-O-silicone bonds, has been reported [27–29].

3.3 X-ray diffraction analysis (XRD)

The diffractograms of each of the analyzed samples (banana starch and starch/silicone composite) are presented in Fig. 4. The X-ray diffraction analysis allowed to verify if the starch granules experienced any effect in its crystalline regions due to silicone. The characteristic peaks of starch 2θ = 15.01 °, 16.89 ° and 23.0 ° and silicone oil at 2θ = 12.69 °, 17.44 ° and 22.50 ° are observed in the diffractogram of Fig. 4. These values are in agreement with those reported by other researchers [20, 30–31].

In the composite starch/silicone the starch peaks are not observed this indicates that the surface of the starch granule was covered by silicon and this diffracts the energy of the X-rays, this suggests that silicone creates a protective barrier and is consistent with the SEM (Fig. 3c and 3d) analysis indicates that starch crystallinity is probably intact in the synthesis of the compound, because the oil protects the surface of the starch. These results agree with those obtained by FTIR and NMR.

3.4 Analysis of pasting

Analysis of the pasting profile of starch and starch/silicone composite is presented in Fig. 5. The starch has a maximum viscosity value of 2.38 Pa.s, which is higher with respect to other sources of starch such as corn (0.075 Pa.s), barley (0.02 Pa.s), mango (0.18 Pa.s), cassava (1.07 Pa.s) reported by other researchers [18, 32].

This is because banana starch has a high amylose content (34.8 %) compared to other sources such as corn (29 %) and potato (21 %), which is known to favor the formation of pasting [33–36]. After the peak of maximum viscosity, a decrease in viscosity was observed due to the collapse of the starch granules. however, during the cooling stage the viscosity increased significantly and was even higher than the maximum viscosity. This behavior is due to the retrogradation of amylose, which forms a network trapping a large amount of water. Starch/silicone composite has a viscosity of 0.052 Pa.s, this value represents a decrease in starch viscosity of 97.81 %. This indicate that the composite granules tend not to swell freely and break in comparison to the starch granules due to the silicon it covers the starch granules, thus preventing the phenomena (swelling, solubility, gelatinization and association of the chains) that occur during the analysis of the pasting profile. These results are consistent with those reported in the literature [37].

3.5 FTIR analysis of films

Infrared spectra of starch and composite films are presented in Fig. 6. From the FTIR spectra of the banana starch film (Film 1) and of the silicone, the characteristic bands of these are observed in the films of the composite.

The vibration signal of the methyl group bonded to silicon (CH_3-Si-) in the composite is observed at 1253 cm^{-1}. This signal is observed from a percentage greater than 5 % of the composite in the formulation of the film. The intensity of this vibration signal increases when the amount of the composite in the film formulation increases, for a percentage equal to 5 % this signal is not observed. A similar behavior shows the vibration signal of the functional group [-O-Si-CH_3], which is clearly observed in 760 cm^{-1} in film 2

and film 3, and in the other films it decreases. From these results it is concluded that the starch/silicone composite is present in the films.

3.6 Thermal properties of films

3.6.1 Differential scanning calorimetry analysis (DSC)

The thermal behavior of the absorption or heat release of the starch/silicone composite film is presented in Fig. 7. The first heat absorption curve observed in the thermogram corresponds to the evaporation of water and the second corresponds to the elimination of glycerol.

Banana starch has a very pronounced heat absorption curve in the range of 300 at 350°C. In all thermograms of the films of the composite this absorption is observed but with varying intensity. This absorption corresponds to the degradation of starch and starch/silicone composite. In all films of the composite, the intensity of this absorption curve increases when the amount of composite increases in the formulation of the film. This indicates the presence of silicone in the starch films generate changes in absorption temperatures.

3.6.2 Thermo gravimetric analysis (TGA)

The thermogravimetric curves (TGA) corresponding to the thermal stability and degradation of the starch and composite film are presented in Fig. 8. The starch thermogram (film 1) has three degradation temperatures at 80, 216 and 307°C corresponding to the decomposition temperatures of water, glycerol and starch, respectively.

The thermogram of the films of the starch/silicone composite is observed at least three degraded products during heating, at 103, 305 and 508°C. These degraded products probably correspond to water, starch and silicone oil, respectively. The temperature at 508°C is observed with a good intensity on the thermogram of film 2 and with a weak intensity on film 3, in the rest of the films it is not observed. This is due these are the films with the highest content of composite in the film, that is, 40 and 20 %, respectively. In films 2 to 5, the starch degradation temperature increases to a value of 328°C. This indicates that the composition provides more thermal stability to the starch. Composite films have a lower residual mass value with respect to starch films (approximately 10 % vs. 19 %).

3.7 X-ray diffraction analysis of films

Diffractograms of the starch/silicone composites films compared to starch and composite (powder) are presented in Fig. 9. The characteristic peaks of the composite appear at 2θ = 12.69 °, 17.30 ° and 22.53 °, and these are not observed in the films of the composite, only those of the starch are observed at 2θ = 15.01 °, 16.91 °, 19.75 °, 22.20 ° and 23.27 °. The intensity of the signals of the composite films are directly proportional to the amount of composite used in the formulation of the film.

Film 2 is the film with the highest amount of composite (40 %) therefore it has peaks with a lower intensity compared to the other films. This result indicates that the presence of the composite in the

starch does not affect its crystallinity up to a percentage of 20 % of this in the film. A similar behavior has been reported in the literature in the preparation of a starch/halloysite composite [38].

3.8 Mechanical properties of films

The determination of the fracture tension (TF), elongation percentage (E) and modulus of elasticity (ME) of the starch film and the starch/silicone composite were carried out, the results are presented in Table 2. Starch/silicone composite has higher values of TF, % E and ME with respect to the starch-only film. The film with the highest values of these three mechanical properties is film 4. This film contains 15% starch/silicone composite and increases by 12.57 % TF, 4.88 % E and 24.51 % ME with respect to the starch-only film.

Table 2
Mechanical properties of starch and composite films.

Film	Fracture tension (MPa)	Elongation percentage (%)	Modulus of elasticity (Mpa)
1	8.83 ± 0.41	25.53 ± 1.59	112.0417 ± 4.34
2	11.42 ± 0.67	27.13 ± 1.10	123.0567 ± 7.60
3	11.09 ± 0.51	28.40 ± 0.91	137.3767 ± 5.11
4	9.94 ± 0.19	26.77 ± 1.41	139.5033 ± 5.69
5	9.01 ± 0.34	24.82 ± 0.76	134.1200 ± 4.01

From the values in Table 2 it is concluded that as the amount of starch/silicone composite decreases, fracture tension and elongation percentage decrease, such is the case of film 5 which contains 10 % of the composite. These results indicate that a better material is obtained with respect to starch-only materials. Therefore, it could be used as a protective film for materials sensitive to oxidation or moisture. On the other hand, these results corroborate the tendency in the intensities of the vibration signals of the FTIR spectra of the functional group -O-Si-CH_3.

3.9 Electrical conductivity of films

The electrical conductivity of starch films and composites are presented in Table 3. The presence of the composite in the starch film favors its electrical conductivity. The film 2 has a value of 0.68 V (40 % of composite in the film) while the film 1 (100 % starch) registers a value of 0.44 V, there is an increase in the electrical conductivity of 54.54 %.

Table 3
Films electrical current values of films.

Film	Electrical conductivity (Voltios)
1	0.44
2	0.68
3	0.60
4	0.53
5	0.47

Films 3, 4 and 5 have voltage values less than that of film 2 but greater than that of film 1. These results indicate that the increase in the value of the electric current is related to the amount of composite used in the formulation of the film. This electrical trend that starch presents with respect to the increase in the concentration of a chemical species in the formulation of its film is similar to that reported in the literature [39–40]. Therefore, it is concluded that this functional group favors the increase in the mechanical properties of the starch/silicone composite films, in their thermal resistance and in its electrical conductivity. From all the results obtained in this investigation, it is proposed as a possible use of the composite as a coating of materials exposed to heat and oxidation for its protection.

4 Conclusions

The synthesis of the starch/silicone composite was carried out. A yield of 84.63 % was obtained for a starch/silicone mass ratio of 2.0, a time of 24 hours and a temperature of 150°C. SEM characterization showed that the starch granules have a granule size of 5 to 50 μ and these were covered in the silicone. Analysis by FTIR and Raman allowed to identify the groups -C-O- and -O-Si-CH_3 of the starch and silicone in the composite. From the analysis by ^{29}Si NMR it was determined that a starch/silicone mixture is obtained.

From the pasting results it was deduced that the granules of the composite tend not to swell freely and break in comparison to the granules of the starch. The films of the composite were elaborate, and it was observed that the homogeneity of these is a function of the amount of compound used in the formulation of the films.

FTIR analysis of the films allowed identifying the characteristic signals of the starch and silicone present in the composite films. From the results of the thermal analysis, it was determined that the starch/silicone composite provides greater thermal stability to the starch. Composite films increase the electrical conductivity of starch by up to 54.54 % and increase the mechanical properties of fracture stress, elongation percentage and modulus of elasticity by 12.57 %, 4.88 % and 24.51 %, respectively.

Declarations

Acknowledgements

We are grateful to University of Papaloapan, University of Guanajuato and Martha Rocio Valencia Estacio for their assistance on this article.

Funding statement

Not applicable

Conflict of Interes

Authors declare no conflict of interest

Author contributions

PGC, RHA and RPG designed and performed the experiments, analysed the results and prepared a write-up; ASA, ACA and GGG performed nuclear magnetic resonance, scanning electron microscopy and X-ray diffraction experiments and data analysis; BGJE, PCDE performed mechanical properties and thermal properties of films.

Availability of data and material

Electronic supplementary material contains a Raman spectrum

Compliance with ethical standards

Not applicable

Consent to participate

Not applicable

Consent for Publication

Not applicable

References

1. Nonhlanhla M, Yahya EC, Pradeep K, Lisa CT, Mershen G, Sunaina I, Viness P (2017) A review of the chemical modification techniques of starch. Carbohydr Polym 157:1226–1236
2. Bhupinder K, Fazilah A, Rajeev B, Alias AK (2012) Progress in starch modification in the last decade. Food Hydrocoll 26:398–404

3. Fan Z (2019) Starch based Pickering emulsions: Fabrication, properties, and applications. Trends Food Sci Technol 85:129–137
4. Shazia T, Muhammad Y, Muhammad AZ, Irfan M, Muzamil M, Aqdas N, Muhammad NI, Khalid MZ (2019) A review on blending of corn starch with natural and synthetic polymers, and inorganic nanoparticles with mathematical modeling. Int J Biol Macromol 122:969–996
5. Awham MH, Bilal AFA (2019) Employment the plastic waste to produce the light weight concrete. Energy Procedia 157:30–38
6. Weizi C, Peipei L, Bin Cn, Haoran X, Zhijun L, Qian Z, Fangyong Y, Meilin L, Meina C, Jiang L, Meng N (2019) Plastic waste fuelled solid oxide fuel cell system for power and carbon nanotube cogeneration. Int J Hydrog Energy 44:1867–1876
7. Hulwani AMZ, Abdul MKW, Hanafi I (2018) Solid-state photo-cross-linking of cassava starch: improvement properties of thermoplastic starch. Polym Bull 75:3341–3356
8. Zhang K, Young SK, Piyawanee J, Suwabun C, Hyoung JC (2017) Stimuli-response of chlorosilane-functionalized starch suspension under applied electric fields. Polym Bull 74:823–837
9. Limei H, Zhanhua S, Xiaopeng Z (2009) Mechanical behavior of starch/silicone oil/silicone rubber hybrid electric elastomer. React Funct Polym 69:165–169
10. Negita K, Itou H, Yakou T (1999) Electrorheological Effect in Suspension Composed of Starch Powder and Silicone Oil. J Colloid Interface Sci 209:251–254
11. Winslow WM (1949) Induced fibration of suspensions. J Appl Phys 20:1137–1140
12. Shaohuang W, Zhonghua L, Yan Z, Lixian C, Jianzhang Z (2009) Facile synthesis of SBA-15/polyaniline nanocomposites with high electrochemical activity under neutral and acidic conditions. React Funct Polym 69:130–136
13. Giselle M, Lincoln S, Mattos D, Guimarães B, Merino E (2019) Ergonomic evaluation of the musculoskeletal risks in a banana harvesting activity through qualitative and quantitative measures, with emphasis on motion capture (Xsens) and EMG. Int J Ind Ergon 69:80–89
14. Rahul T, Penta P, Michael B, Sukhvinder PS, Christopher JS, Costas ES, Quan VV (2019) A starch edible surface coating delays banana fruit ripening. LWT Food Sci Techol 100:341–347
15. Aparicio-Saguilán A, Aguirre-Cruz A, Méndez-Montealvo G, Rodriguez-Ambriz SL, Garcia-Suarez FL, Páramo-Calderón DE, Bello-Pérez LA (2014) The effect of the structure of native banana starch from two varieties on its acid hydrolysis. LWT- Food Sci Techol 58:381–386
16. Agama-Acevedo E, Islas-Hernandez JJ, Osorio-Díaz P, Rendón-Villalobos R, Utrilla-Coello G, Angulo R, Bello-Pérez O LA (2009) Pasta with unripe banana flour: physical, texture, and preference study. J Food Sci 74:263–267
17. Ramírez-Hernández A, Mata-Mata JL, Aparicio-Saguilán A, González-García G, Hernández-Mendoza H, Gutiérrez-Fuentes A, Báez-García E (2016) The effect of ethylene glycol on starch-g-PCL graft copolymer synthesis. Starch/starke 11:1148–1157

18. Tecante A, Doublier JL (1999) Steady flow and viscoelastic behavior of crosslinked waxy corn starch-κ-carrageenan pastes and gels. Carbohydr Polym 40:221–231
19. ASTM D882-95a (1995) Standard test method for tensile properties of thin plastic sheeting. ASTM International, Philadelphia. https://www.astm.org/Standards/D882
20. Ramírez-Hernández A, Aparicio-Saguilán A, Reynoso-Meza G, Carrillo-Ahumada J (2017) Multi-objective optimization of process conditions in the manufacturing of banana (Musa paradisiaca L.) starch/natural rubber films. Carbohydr Polym 157:1125–1133
21. Kordian C, Marcin S, Piotr J, Lesniak M, Maciej S, Jacek F (2018) Spectroscopic studies of the silicone oil impact on the ophthalmic hydrogel based materials conducted in time dependent mode. Spectrochimica Acta A Molecular Biomol Spectroscopy 192:1–5
22. Österle W, Gradt AG, Häusler T, Rossi I, Wetzel A, Zhang B, Dmitriev G AI (2015) Exploring the potential of Raman spectroscopy for the identification of silicone oil residue and wear scar characterization for the assessment of tribofilm functionality. Tribol Int 90:481–490
23. Galvis L, Bertinetto CG, Jean-Luc P, Montesanti N, Vuorinen T (2016) Crystallite orientation maps in starch granules from polarized Raman spectroscopy (PRS) data. Carbohydr Polym 154:70–76
24. Łabanowska M, Wesełucha-Birczyńska A, Kurdziel M, Puch P (2013) Thermal effects on the structure of cereal starches. EPR and Raman spectroscopy studies. Carbohydr Polym 92:842–848
25. Núñez-Santiago MC, Bello-Pérez LA, Tecante A (2004) Swelling-solubility characteristics, granule size distribution and rheological behavior of banana (Musa paradisiaca) starch. Carbohydr Polym 6:65–75
26. Montoya J, Dumar Q, Lucas J (2015) Characterization of starch and flour of Gros Michel banana fruit (Musa acuminata AAA). Acta Agron 64:11–21
27. Ueda T, Takagi S, Nishida M, Hishiki N, Ogura (1987) Nippon Starch Chemical Co., Jpn. Kokai Tokkyo Koho, Japanese Patent No. 62218401
28. Sébe G, Brook MA (2001) Hydrophozation of wood Surfaces: Covalent grafting of silicone polymers. Wood Sc Technol 35:269–282
29. Brook MA, Jiang J, Heritage P, Underdow B, McDermott MR (1997) Silicone-modified starch/protein microparticles: protecting biopolymers with a hydrophobic coating. Colloids Surf B Biointerfaces 9:285–295
30. Fang J, Fowler P, Sayers C, Williams P (2004) The chemical modification of a range of starches under aqueous reaction conditions. Carbohydr Polym 55:283–289
31. Ramírez-Hernández A, Mata-Mata JL, Aparicio-Saguilán A, González-García G, Hernández-Mendoza H, Gutiérrez-Fuentes A, Báez-García E (2016) Chemical modification of banana starch by the in situ polymerization of ϵ-caprolactone in one step. Starch/starke 69:1–10
32. Yongtao Y, Xiaojuan X, Qiang W (2021) Effects of potassium sulfate on swelling, gelatinizing and pasting properties of three rice starches from different sources. Carbohydr Polym 251:117057

33. Daisuke H, Yasutaka T, Kazuya Y, Jun-ichi K (2014) Hierarchically self-assembled nanofiber films from amylose-grafted carboxymethyl cellulose. Fibers 2:34–44
34. Palviainen P, Heinämäki J, Myllärinen P, Lahtinen R, Yliruusi J, Forssell P (2001) Corn starches as film formers in aqueous-based film coating. Pharm. Dev. Technol. 2001, 6, 353–361
35. Hongyan L, Minghao X, Shu Y, Ruoxin L, Zichu M, Yangyang W, Jing W, Baoguo S (2020) Insights into waxy maize starch degradation by sulfuric acid: Impact on starch structure, pasting, and rheological property. Int J Biol Macromol 165:214–221
36. Bello-Perez LA, Aparicio-Saguilán A, Mendez-Montealvo G, Solorza-Feria J, Flores-Huicochea E (2005) Isolation and partial characterization of mango (Magnifera indica L.) starch: morphological, physicochemical and functional studies. Plant Food Hum Nutr 60:7–12
37. Mali S, Ferrero C, Redigonda V, Beleia AP, Grossmann MVE, Zaritzky NE (2003) Influence of pH and hydrocolloids addition on yam (Dioscorea alata) starch pastes stability. LWT Food Sci Technol 36:475–481
38. Ren J, Dang KM, Pollet E, Avérous L (2018) Preparation and Characterization of Thermoplastic Potato Starch/Halloysite Nano-Biocomposites: Effect of Plasticizer Nature and Nanoclay Content. Polímers 10:808–823
39. Shadpour M, Shima R (2017) Starch/MWCNT-vitamin C nanocomposites: Electrical, thermal properties and their utilization for removal of methyl Orange. Carbohydr Polym 169:23–32
40. González K, García-Astrain C, Santamaria-Echart A, Ugarte L, Avérous L, Eceiza A, Gabilondo N (2018) Starch/graphene hydrogels via click chemistry with relevant electrical and antibacterial properties. Carbohydr Polym 202:372–381
41. Karrasch A, Wawrzyn E, Schartel B, Jäger C (2010) Solid-state NMR on thermal and fire residues of bisphenol A polycarbonate/silicone acrylate rubber/bisphenol A Bis(diphenyl-phosphate) (PC/SiR/BDP) and PC/SiR/BDP/zinc borate (PC/SiR/BDP/ZnB) — Part II: The influence of SiR. Polym Degrad Stabil 95:2534–2540

Figures

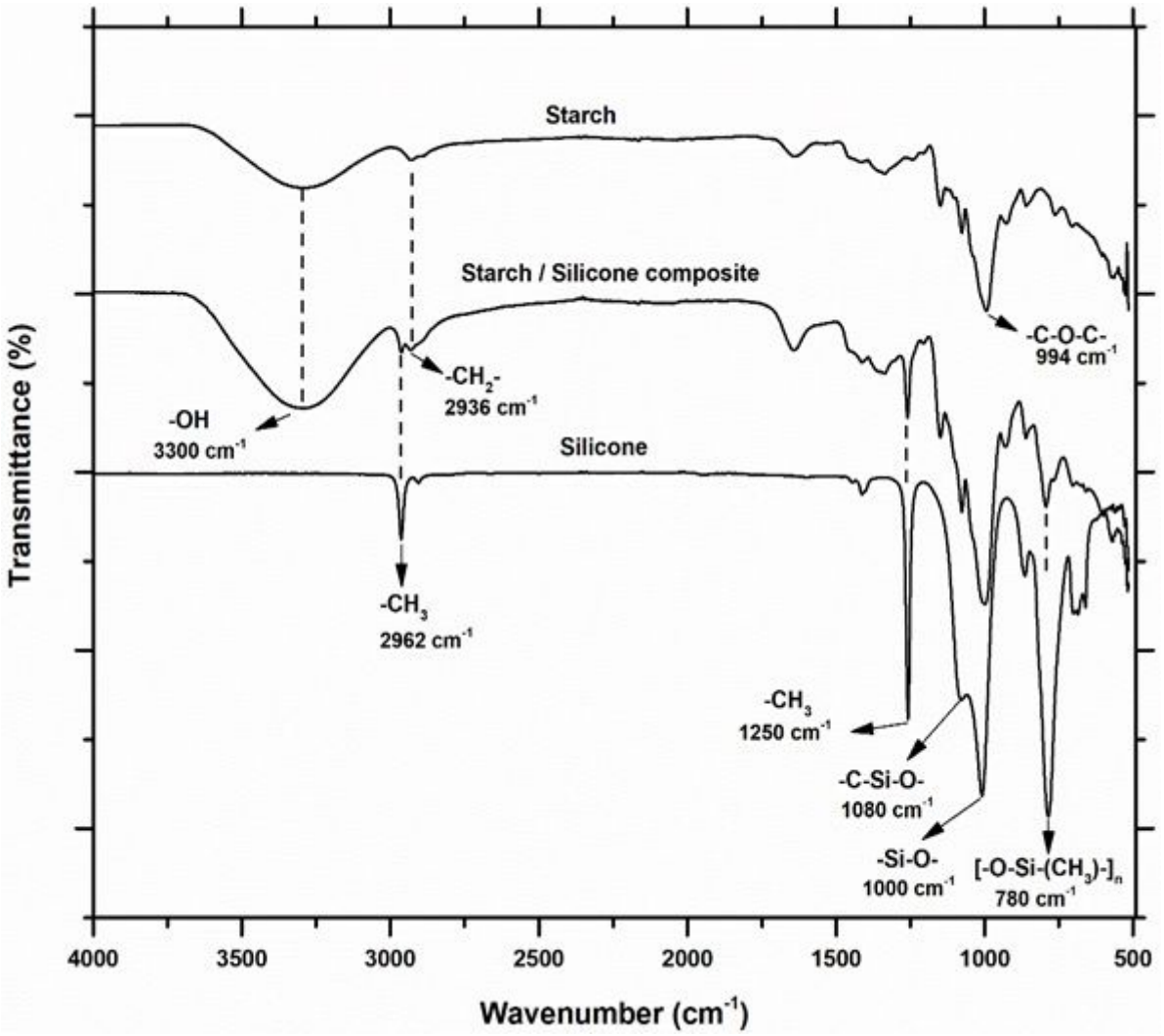

Figure 1

FTIR spectra of banana starch, silicone and starch/silicone composite.

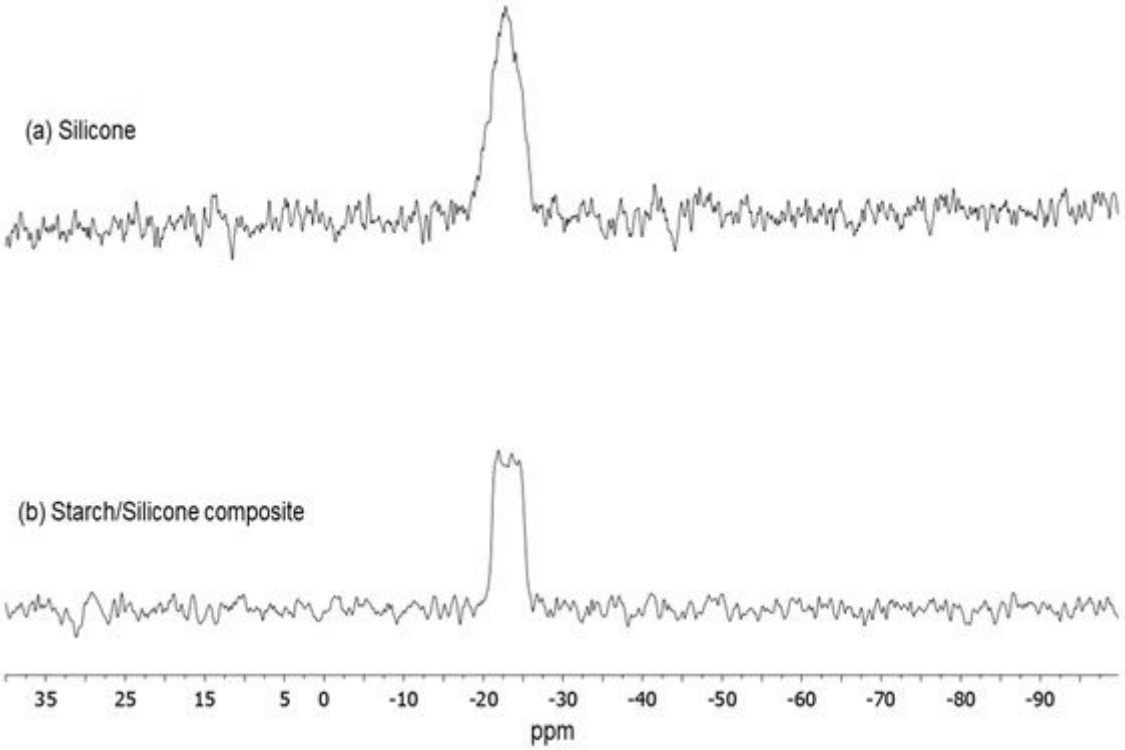

Figure 2

29Si NMR of banana starch and starch/silicone composite.

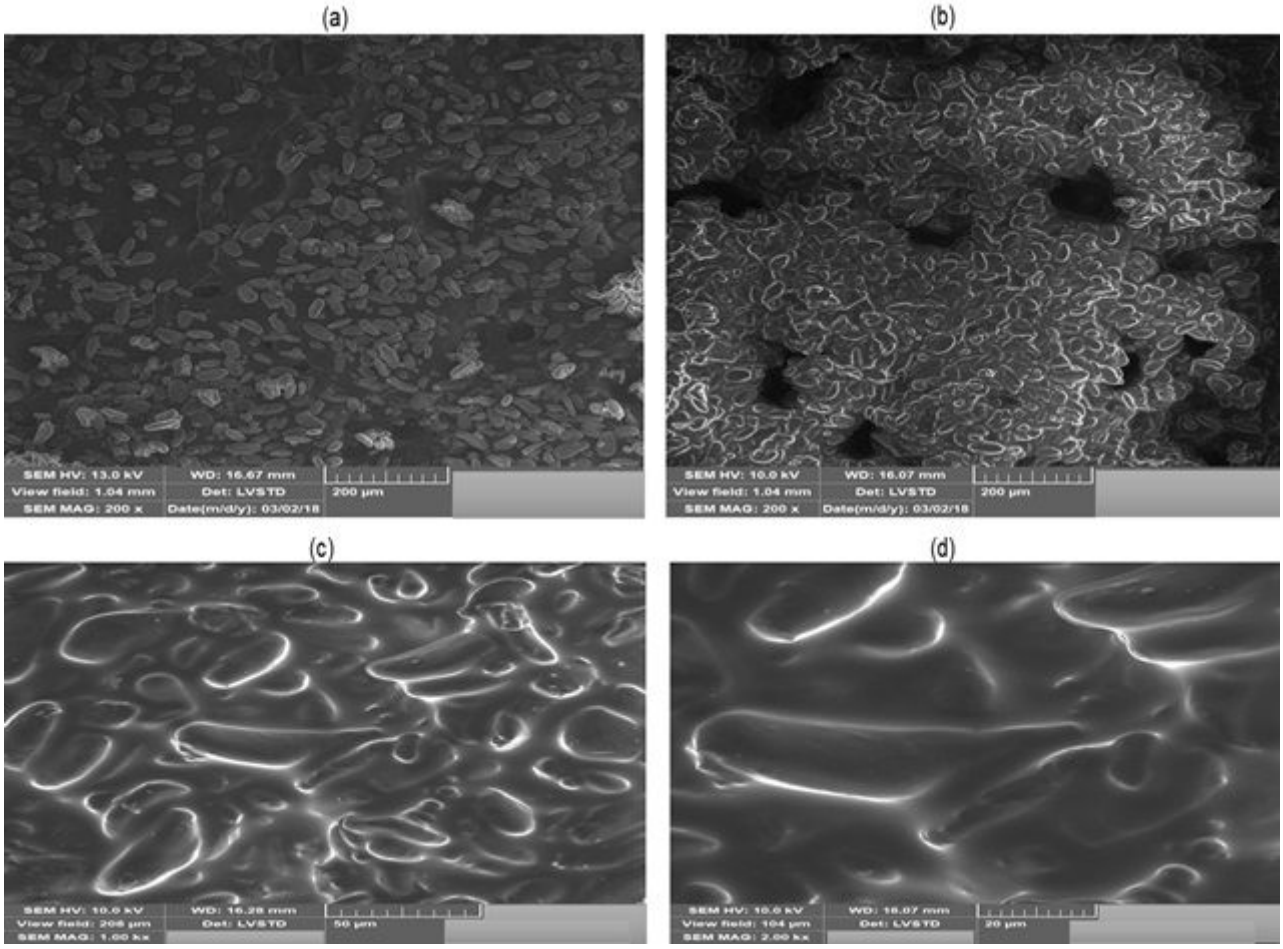

Figure 3

SEM micrograph of banana starch (a) and starch/silicone composite (b, c, d) at different resolution scales (200x and 1.0 kx).

Figure 4

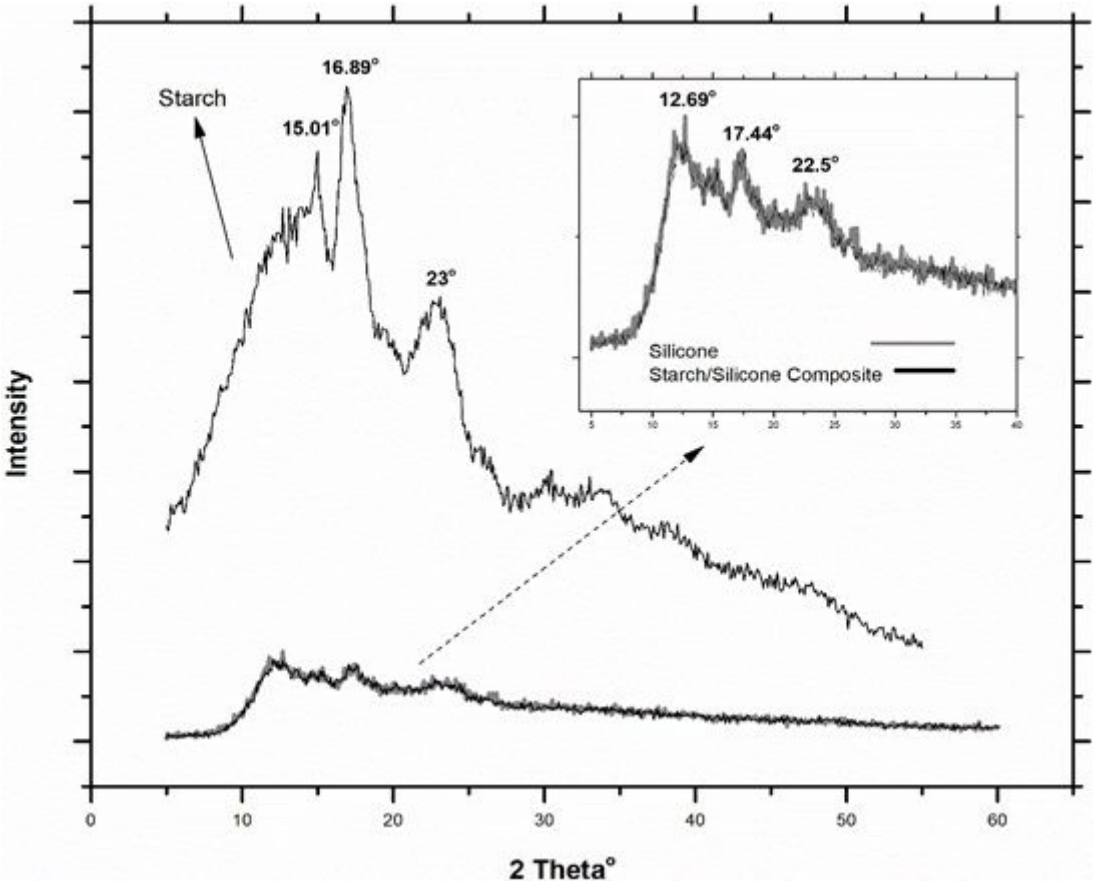

X-ray diffraction patterns of banana starch and starch/silicone composite.

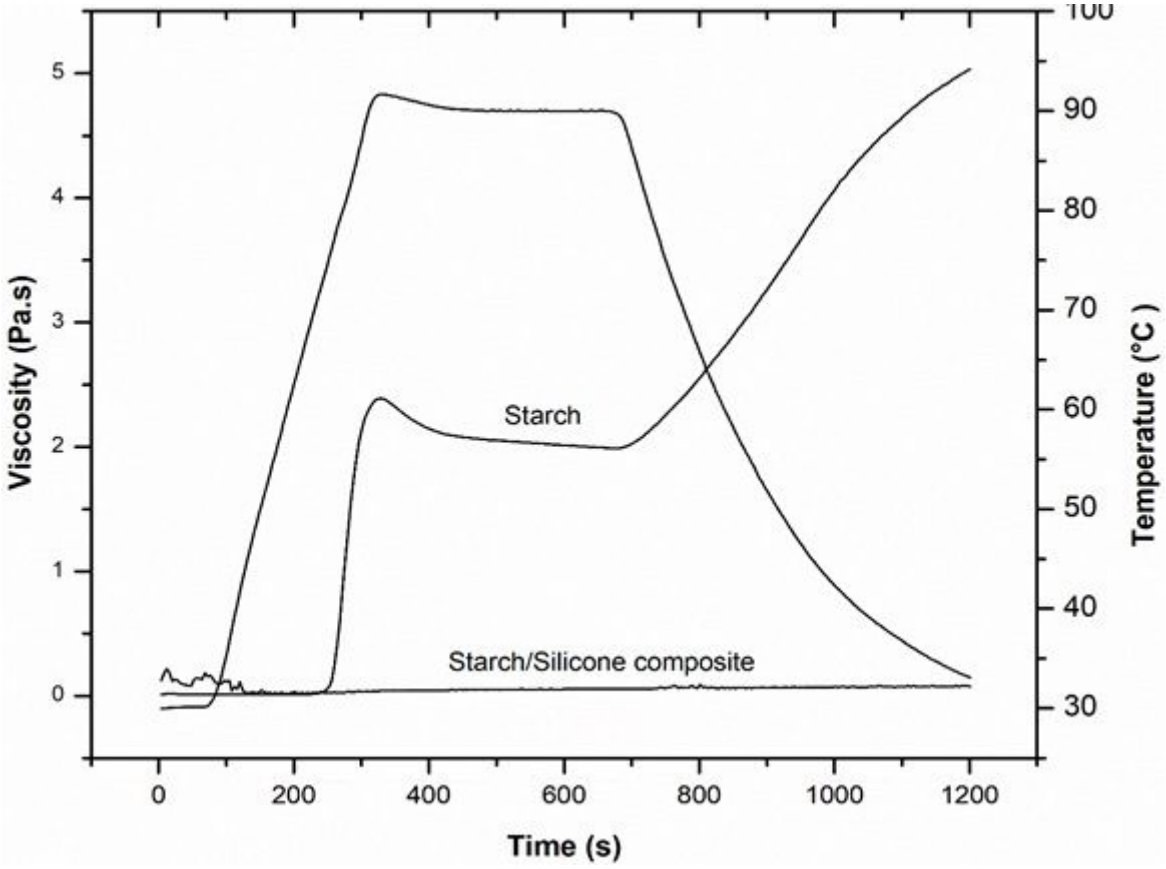

Figure 5

Pasting of banana starch and starch/silicone composite.

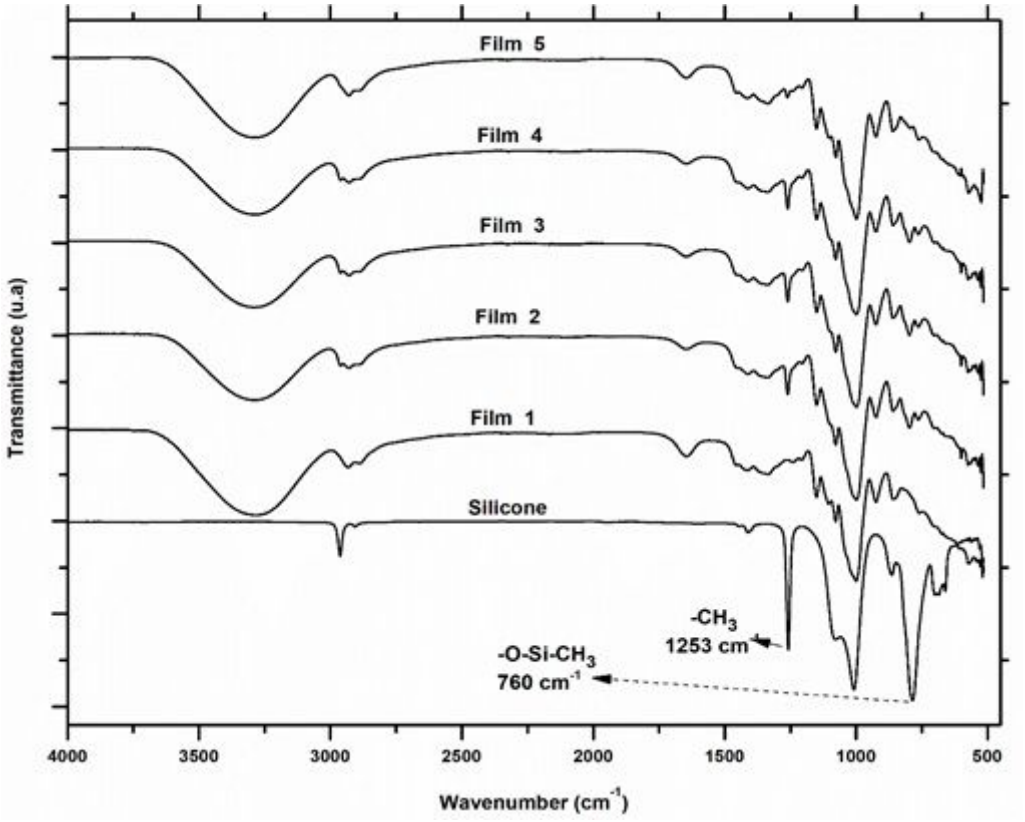

Figure 6

FTIR spectra of composite films and silicone.

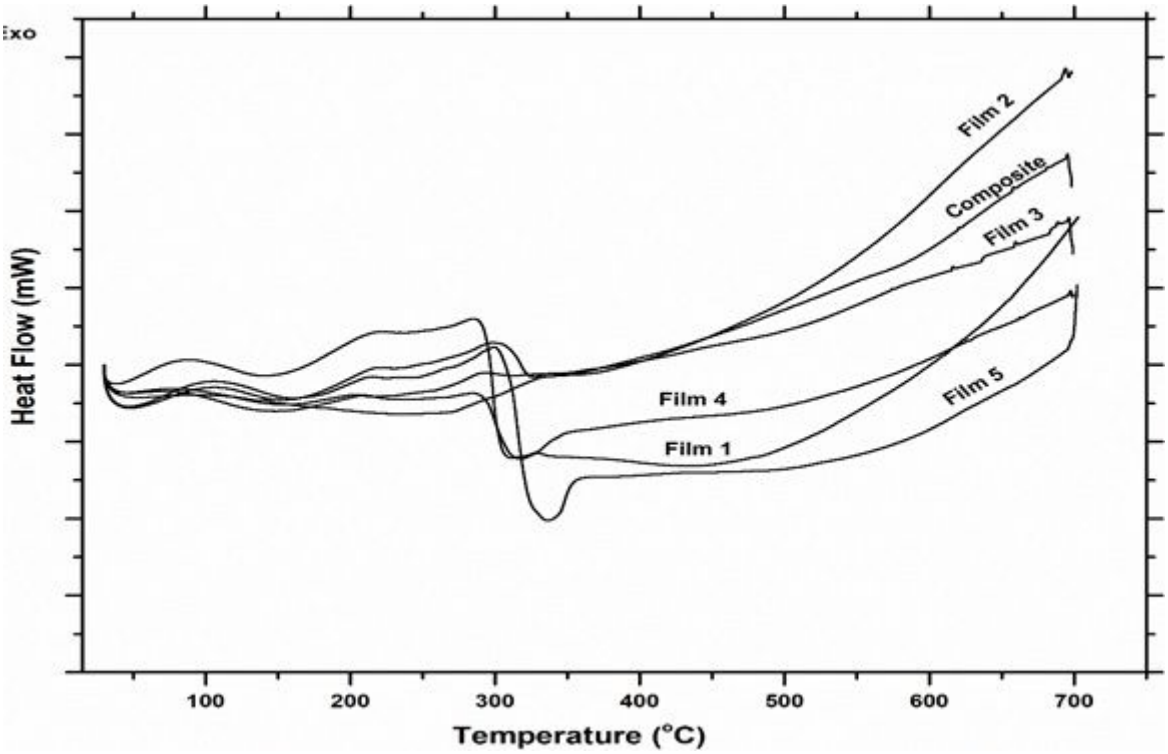

Figure 7

DSC thermogram of starch and composite films.

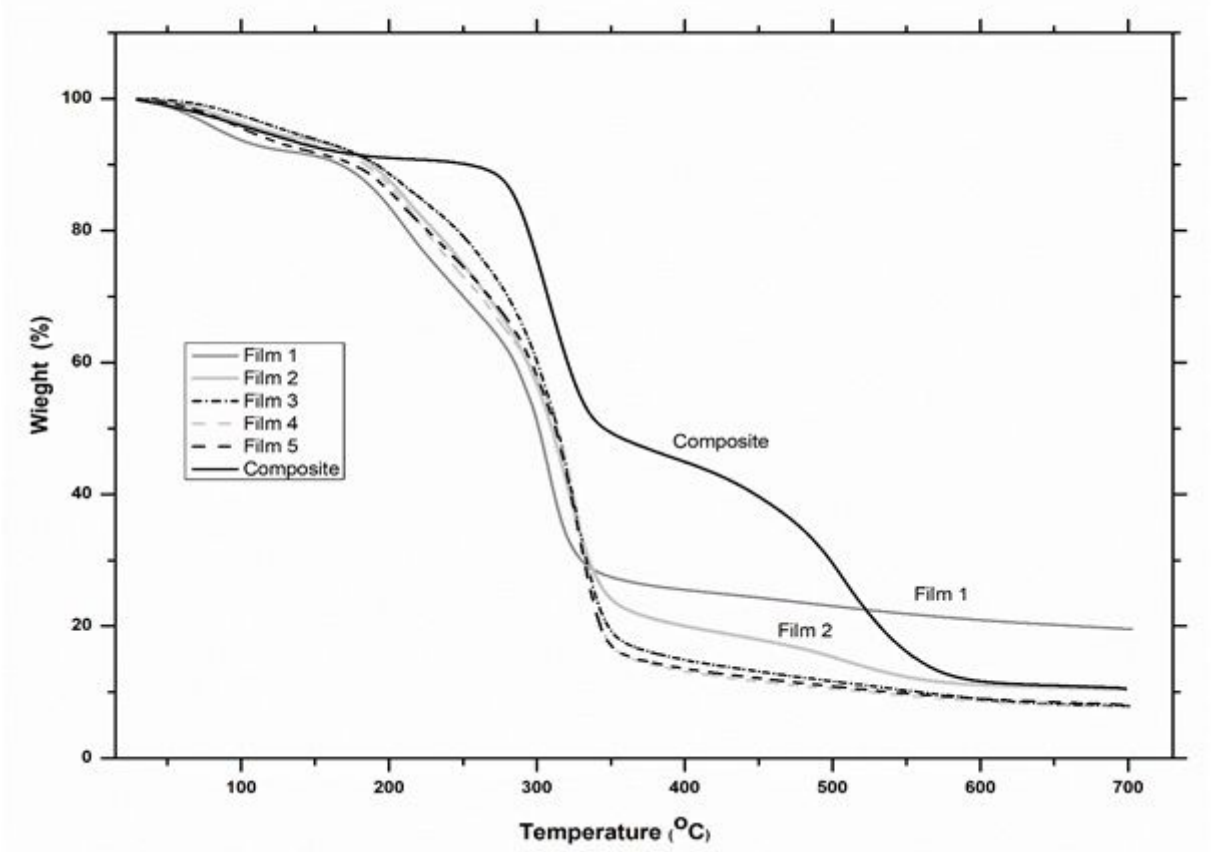

Figure 8

TGA thermograms of starch film and composite films

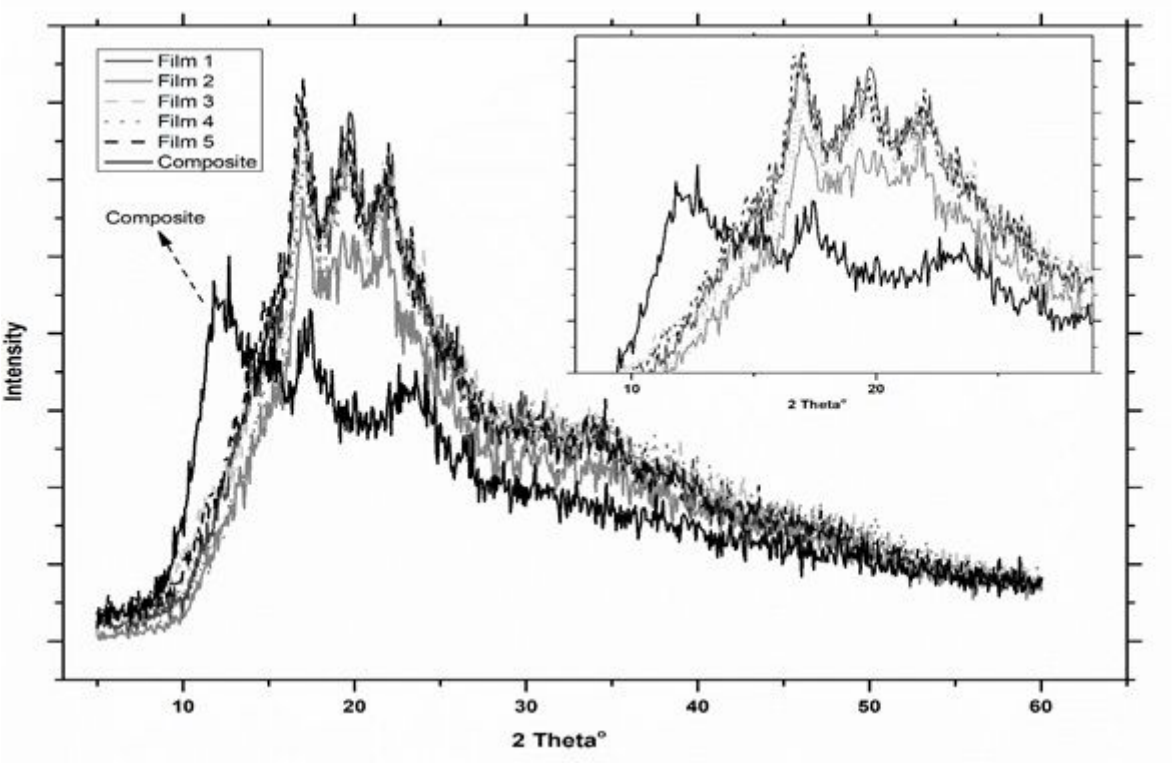

Figure 9

X-ray diffractogram of starch film and composite films.

Supplementary Files

This is a list of supplementary files associated with this preprint. Click to download.

- Suplem.docx